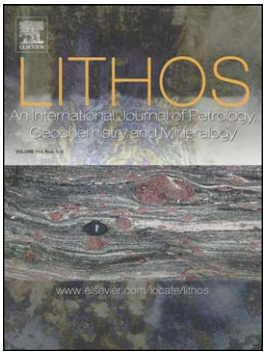

Petrogenesis of Triassic granitoids in the East Kunlun Orogenic Belt, northern Tibetan Plateau and their tectonic implications

Fengli Shao, Yaoling Niu, Yi Liu, Shuo Chen, Juanjuan Kong, Meng Duan

PII: S0024-4937(17)30088-9
DOI: doi:10.1016/j.lithos.2017.03.002
Reference: LITHOS 4251

To appear in: *LITHOS*

Received date: 27 August 2016
Accepted date: 2 March 2017

Please cite this article as: Shao, Fengli, Niu, Yaoling, Liu, Yi, Chen, Shuo, Kong, Juanjuan, Duan, Meng, Petrogenesis of Triassic granitoids in the East Kunlun Orogenic Belt, northern Tibetan Plateau and their tectonic implications, *LITHOS* (2017), doi:10.1016/j.lithos.2017.03.002

Petrogenesis of Triassic granitoids in the East Kunlun Orogenic Belt, northern Tibetan Plateau and their tectonic implications

Fengli Shao [a, b,c,*], Yaoling Niu [a,b,d,*], Yi Liu [e], Shuo Chen [a ,b,c], Juanjuan Kong [a ,b,c], Meng Duan [e]

[a] Institute of Oceanology, Chinese Academy of Sciences, Qingdao 266071, China

[b] Laboratory for Marine Geology, Qingdao National Laboratory for Marine Science and Technology, Qingdao 266061, China

[c] University of Chinese Academy of Sciences, Beijing 100049, China

[d] Department of Earth Sciences, Durham University, Durham DH1 3LE, UK

[e] School of Earth Science and Resources, China University of Geosciences, Beijing 100083, China

* Corresponding authors:
Institute of Oceanology, Chinese Academy of Sciences, 7# Nanhai Road, Shinan District, Qingdao 266071, China. Tel.:+86 15652927971
E-mail address: Miss Fengli Shao (fenglishao@126.com)
Professor Yaoling Niu (yaoling.niu@durham.ac.uk)

Abstract

The East Kunlun Orogenic Belt (EKOB), an important part of the Greater Tibetan Plateau, is an ideal region for understanding the tectonic evolution of the Anyemaqen Ocean. Here, we present zircon U-Pb ages, bulk-rock major and trace element analyses and Sr-Nd-Hf isotope compositions on representative samples of the syn-collisional Dulan batholith at the eastern end of the EKOB. The zircon U-Pb age data indicate that the bulk of the Dulan batholith was emplaced at 240-235 Ma. The granitoids have high- to medium-K and metaluminous characteristics. They are enriched in large ion lithophile elements (LILEs) and light rare earth elements (LREEs) and depleted in some high field strength elements (HFSEs, e.g., Nb and Ta), while having a flat heavy REE (HREEs) pattern. The mafic magmatic enclaves

(MMEs) share the same age, mineralogy and indistinguishable Sr-Nd-Hf isotopes with their granitoid hosts except for the higher HREE abundances. We show that the MMEs represent cumulate formed at earlier stages of the same magmatic system. The trace element data (e.g., Nb/Th, Ta/U) and inherited mantle isotopic characteristics of the Dulan batholith are also consistent with an origin via partial melting of the last fragments of underthrusting ocean crust. Simple mass balance calculations using the Sr-Nd-Hf isotopic data show that ~ 85% Paleo-Tethys MORB and ~15% mature crustal material (the Proterozoic gneiss of the study area) contribute to the source of the granitoids. The Dulan batholith shows compositional similarities to the bulk continental curst with inherited mantle isotopic signatures. The syn-collisional felsic magmatism must have contributed to the net continental crust growth in the EKOB. We infer that the Kunlun and Qinling orogens may actually be one single orogen offset later by the Wenquan fault system.

Keywords:

East Kunlun; Granitoids; Dulan batholith; Syn-collisional; Continental crust growth

1. Introduction

The Greater Tibetan Plateau is a geological amalgamation that comprises a number of accreted blocks separated by suture zones (Fig. 1a). The continental collision events are progressively younger from northeast since the Early Paleozoic (e.g., ~ 450 Ma, the North Qilian Orogen; Huang et al., 2015; Song et al., 2007, 2013; Xu et al., 2010; Yang et al., 2015) to southwest in the Cenozoic (e.g., ~ 55 Ma, Yarlu-Zangbo suture; He et al., 2007; Mo et al., 2005; Ji et al., 2009; Lee et al., 2009;

Zhu et al., 2015). Hence, the Greater Tibetan Plateau is also known as "Orogenic Plateau" (Xu et al., 2007). The syn-collisional granitoids and volcanic rocks in the Lhasa Terrane (Fig. 1a) are well studied (e.g., Dai et al., 2015; Kang et al., 2009; Mo et al., 2003, 2005, 2007, 2008; Ji et al., 2009; Ravikant et al., 2009; Sun et al., 2015; Wen et al., 2008), while the research on the northern collisional zones is relatively limited. The East Kunlun Orogenic Belt (EKOB), which is in the northern part of the Greater Tibetan Plateau, contains voluminous syn-collisional felsic rocks and records the history of the Anyemaqen Ocean (Chen et al., 2015a; Hu et al., 2015; Huang et al., 2014; Liu et al., 2015; Xia et al., 2014). Most importantly, the EKOB is an important component of the Central Orogenic Belt of China (Jiang, 1993; Yin and Zhang; 1998) and lies at the triple junction of the Kunlun, Qinling and Qilian orogenic belts (Fig. 1b). It is an ideal site to discuss the tectonic evolution of these orogens.

Based on the research of syn-collisional granitoid rocks which show remarkable compositional similarity to the bulk continental crust in the Lhasa Terrane (also called Gangdese magmatic belt), Niu et al. (2013) hypothesized that continental collision zones are primary sites of net continental crustal growth. This hypothesis overcomes the shortcomings of the standard "island-arc model" (i.e., continental crust is produced through subduction-zone magmatism; Taylor, 1967). Comparisons between "continental collision zone model" and "island-arc model" were discussed in detail by Niu and O'Hara (2009) and Niu et al (2013). The East Kunlun magmatic belt is the only one that is comparable with the Gangdese magmatic belt on the Greater Tibetan Plateau (Mo et al., 2007). Hence, the EKOB is another ideal site to test the hypothesis of the "continental collisional zone model" for continental crust growth (Huang et al., 2014; Mo et al., 2008; Niu and O'Hara, 2009; Niu et al., 2013).

We use the petrology, geochronology, whole-rock major and trace element compositions and Sr-Nd-Hf isotopic data to constrain the petrogenesis of the Dulan batholith in the context of the tectonic evolution of the EKOB.

2. Geology and samples

The Kunlun orogen is divided into West Kunlun and East Kunlun by the sinistral strike-slip Altyn Tagh fault. The East Kunlun orogenic belt stretches out about 1500 km and adjoins the West Qinling orogenic belt to the east. The EKOB has a north-south extension for 50-200 km with the Qaidm basin to the north and Songpan-Garze terrane to the south. It can be divided into three tectonic zones on the basis of the major faults (Fig. 1c; Yang et al., 1996; Xu et al., 2011; Xia et al., 2015). The oldest basement of the EKOB is the Paleoproterozoic Mohe gneiss of the Jinshuikou Group that cropped out to the southeast of Xiangride town (~2390 Ma, Ba et al., 2012; Gong et al, 2012; Hao et al., 2004). The EKOB preserves geological records of the early Paleozoic Caledonian cycles and the late Paleozoic to early Mesozoic Variscan-Indosinian cycle. The Early Paleozoic granitoids (500-400 Ma) are comparable with those in the North Qilian orogenic belt (see Appendix Table 1 of Mo et al., 2007). The Permian-Triassic granitoids are dominant in the EKOB (~25000 km^2) and account for 50% of the total outcrop area of the granitoids (Luo et al., 2002). These granitoids, which mainly display in North East Kunlun and Central East Kunlun (Fig. 1c), are exposed as large-scale linear plutonic complexes (Fig. 2).

The Dulan batholith (~ 235 Ma, ~ 900 km^2; Fig. 2) is located at the east end of the EKOB. It has an additional northward extension (~ 100km; 1: 250 000 Dulan geological map sheet, Tianjin Center of Geological Survey, 2003), making the EKOB look like a rotated letter “b” (Fig. 1b). The Triassic Dulan batholith (240-235 Ma)

intrude the Mesoproterozoic Xiaomiao formation and Paleoproterozoic Baishahe formation. Mafic magmatic enclaves (MMEs; Fig. 3a, b), which are abundant in the collisional plutons (Chen et al., 2015b; 2016; Liu et al., 2003, 2004; Liu et al., 2015; Luo et al., 2014; Xia et al., 2014, 2015), are common in the Dulan batholith.

We collected 29 representative samples, including 22 granitoid hosts, 5 MMEs and 2 granitic gneisses from 24 locations (Fig. 2; Appendix Table 1) along the major river valleys cross-cutting the Dulan batholith. These granitoids are medium-coarse grained and consist of quartz (30-35%), plagioclase (35-40%), K-feldspar (15-20%), amphibole (10-15%), biotite (< 5%) and accessory minerals such as apatite, magnetite and zircon (Fig. 3). The evolved granite DLX12-07 (SiO_2 = 75.57 wt. %) is pinkish, fine-medium grained and contains more quartz (35-40%) and K-feldspar (20-25%). The MMEs are fine grained and have the same mineralogy as their hosts, but higher modes of mafic phases (e.g., amphibole and biotite). The MMEs are usually lenticular and undergoing plastic deformation.

3. Analytical methods

We cut the hand specimen into 1cm-thick pieces to ensure all the faces are fresh with saw marks grinded off. The samples were then crushed into 1-2 cm fragments using a percussion mill. The fragments were then ultrasonically cleaned in Milli-Q water, dried, and powdered into 200-mesh. Because the granitoids are coarse-grained, we grind up to ~ 500 g powder to ensure representativeness of the rock samples.

3.1 Zircon U-Pb dating and trace elements

Zircon cathodoluminescence (CL) and reflected-light images were done at China University of Geoscience, Wuhan (CUGW), where U-Pb dating and trace element analysis were carried out simultaneously using LA-ICP-MS. The diameter of the

193nm excimer later ablation spot was ~32μm. For U-Pb dating, natural zircon standard 91500 (Wiedenbeck et al., 1995) was used as external standard while another zircon standard GJ-1 was used as internal standard. For trace element analysis, ^{29}Si of U.S. Geological Survey (USGS) reference materials (BCR-2G and BIR-1G) were used as the external standards and silicate glass NIST SRM 610 was analyzed to optimize the instrument. Detailed operating conditions and analytical precisions for the LA-ICP-MS were described in Liu et al. (2008, 2010). Common Pb correction and age calculation were done using *ComPbCorr#3.15* (Andersen, 2002) and *Isoplot/Ex_ver3* (Ludwig, 2003), respectively.

3.2 Major and Trace elements

Bulk-rock major elements were determined using a Leeman Prodigy ICP-OES system at China University of Geosciences, Beijing (CUGB). The USGS standard AGV-2 and two Chinese national geological standards GSR-1 and GSR-3 were used to monitor the analytical accuracy (± 5%, see Supplementary Table 1) and precision (1σ, < 2.0%).

Trace elements were done on an Agilent-7500a ICP-MS at CUGB. About 35 mg powdered sample was dissolved in equal mixture of concentrated HNO_3 and HF with a digesting Teflon vessel and the high-pressure bomb for 48h. Similar procedure was repeated using concentrated HNO_3 for a further 24h. The digested samples were then diluted into 2% HNO_3 solutions and analyzed using ICP-MS. AGV-2 and GSR-1 were used to monitor the analytical accuracy and precision (Supplementary Table 2). Analytical accuracy is better than 5% for most elements and 6-10% for Cu, Y, Dy, Ho and U.

3.3 Bulk-rock Sr-Nd-Hf isotopes

Bulk-rock Sr-Nd-Hf isotope analysis was done in the Guangzhou Institute of Geochemistry, Chinese Academy of Science. About 100 mg sample powder was dissolved with concentrated HNO_3 and HF mixture. Sr was first separated using Sr-Spec resin. AG50W-X12 resin was used to separate high field strength elements (HFSEs) and rare earth elements (REEs). Nd was separated using a conventional di-(2-ethylhexyl) hydrogen phosphate (HDEHP) method and Hf was separated by Ln-Spec resin using the procedure following Li et al. (2005). Isotopic ratios were determined using MC-ICP-MS and corrected for mass fractionation using $^{86}Sr/^{88}Sr$ = 0.1194, $^{146}Nd/^{144}Nd$ = 0.7219 and $^{179}Hf/^{177}Hf$ = 0.7325, respectively. Repeated analysis of USGS standards BCR-2, BHVO-2 and JB-3 gives values consistent with the recommended values (Supplementary Table 3). The mean values for NBS987 Sr standard and Jndi-1 Nd standard yielded $^{87}Sr/^{86}Sr = 0.710279 \pm 29$ (2σ, n = 22) and $^{143}Nd/^{144}Nd = 0.512086 \pm 14$ (2σ, n = 11), respectively. Multiple analyses of BHVO-2 and JB-3 give average $^{176}Hf/^{177}Hf$ of 0.283099 ± 15 (2σ, n = 13) and 0.283216 ± 15 (2σ, n = 6), respectively.

4. Results

4.1 Zircon U-Pb dating and trace elements

The zircons are colorless to pale brown, euhedral to subhedral with clear prisms and pyramids and have distinct oscillatory zonings (Fig. 4i). Some zircon cores display clear “sandglass structure” (e.g., RSX12-34MME-3; Fig. 4i; Wan et al., 2011; Xue et al., 2010). The zircons have varying Th (51-693 ppm) and U (116-1109 ppm) with Th/U ratios of 0.40-0.98 (see Supplementary Table 4), consistent with being of magmatic origin (Hoskin and Schaltegger, 2003).

The Concordia ages of four granitoid and two MME samples indicate that the batholith was emplaced in the time frame of 240-235 Ma (see Fig. 4). It is worth noting that the MMEs have identical ages with their granitoid hosts. Meanwhile, we also analyzed zircons of the granitic gneiss (RSX12-12; Fig. 4h) of the Paleoproterozoic basement (i.e., Baishahe formation) in the East Kunlun (1: 250 000 Dulan geological map sheet). The data show that two of the oldest zircons are ~2.1Ga. This metamorphic age is important for the basement histories, but is beyond the scope of this paper.

4.2 Major and trace elements

The total alkalis *vs.* silica (TAS) diagram (Fig. 5a) shows that the Dulan batholith samples are mostly granodiorite with subordinate granite and diorite. Sample XRD12-06MME plots in the boundary region of gabbroic and dioritic rocks, but they are amphibole-rich dioritic rocks without clinopyroxene (nor orthopyroxene). Most of the samples are metaluminous (A/NK > 1, A/CNK < 1; Fig. 5b). On SiO_2-variation diagrams (Fig. 6), the granitoids define trends resembling liquid lines of decent (LLDs; except Na_2O). Sample XRD12-06MME whose SiO_2 is lowest has lower Al_2O_3, but higher Fe_2O_3, CaO, MgO and MnO. This is consistent with its high modal amphibole (~ 50%). According to the K_2O vs. SiO_2 diagram (Fig. 6h), the granitoids are High-K to Medium-K Calc-alkaline series.

Both granitoids and MMEs are light REE (LREE) enriched (Fig. 7a) with $[La/Yb]_N$ up to 46.74 (RSX12-22 host). The high abundances and flat heavy REE (HREE) patterns are consistent with these samples having no garnet involved in their petrogenesis. The HREE contents of the MMEs are higher than the hosts because of greater proportions of mafic phases (e.g., amphibole and biotite; Chen et al., 2015b, 2016). The evolved sample DLX12-07 has a large negative Eu anomaly (Eu/Eu* =

0.20; Fig. 7a) as the result of significant plagioclase crystallization (also negative Ba, Sr anomalies; see Niu and O'Hara, 2009). Figure 7b shows that the high field strength elements (HFSE) Nb (*vs.* Th) and Ta (*vs.* U) display obvious negative anomalies with Nb* and Ta* values ($Nb^* = [Nb/Th]_{Sample}/[Nb/Th]_{PM}$, $Ta^* = [Ta/U]_{Sample}/[Ta/U]_{PM}$, after Niu and Batiza, 1997; Niu et al., 1999) resembling that of bulk continental crust (BCC, Rudnick and Gao, 2003; Fig. 8). The average composition of the granitoids shows remarkable similarity to the bulk continental crust (Fig. 7b).

4.3 Bulk-rock Sr-Nd-Hf isotopes

The $^{87}Sr/^{86}Sr$ of the granitoids and MMEs have restricted values (0.71001-0.71469), but the evolved granite DLX12-07 has a very high $^{87}Sr/^{86}Sr$ ratio of 0.793407 (Fig. 9a; Appendix Table 3) because of the high Rb/Sr ratio due to significant plagioclase (and alkali feldspars to some content) crystallization, resembling peralkaline rhyolites (Shao et al., 2015). Compared with Nd isotopes ($\varepsilon_{Nd}(t) = -6.40$ to -5.10, t = 235 Ma, this study; Figs. 10a, c), Hf isotopes are more depleted ($\varepsilon_{Hf}(t) = -0.83$ to $+3.68$). The host granitoids and their MMEs have indistinguishable Sr-Nd-Hf isotopes. As expected, Nd-Hf isotopes should correlate with each other and can be explained by the mantle array which is expected to result from mixing of an enriched component and the depleted mantle (i.e., $\varepsilon_{Hf} = 1.59*\varepsilon_{Nd} + 1.28$; Fig. 11b; Chauvel et al., 2008; Zindler and Hart, 1986). However, the ε_{Hf} value of the EKOB granitoids is higher at a given ε_{Nd} value. Huang et al (2014) has discussed the possibility that the elevated $^{176}Hf/^{177}Hf$ may be caused by incomplete digestion of zircons because most of the Zr (also Hf, because of the similar element behavior of them) resides in zircons. Figure 9d shows that the Lu-Hf pseudio-isochron age is 424 Ma. This age is much higher than the zircon U-Pb ages (~235-240 Ma)

while the Rb-Sr and Sm-Nd pseudio-isochron ages are similar to the zircon U-Pb ages (Figs. 9a-c).

In addition, the $^{87}Sr/^{86}Sr$ of the granitic gneiss (RSX12-12) is 0.750347, and the $^{143}Nd/^{144}Nd$ and $^{176}Hf/^{177}Hf$ are 0.511662 and 0.282232 respectively (Initial $^{87}Sr/^{86}Sr$ = 0.73802, $\varepsilon_{Nd}(t)$ = -17.0, $\varepsilon_{Hf}(t)$ = -15.5, t = 235 Ma, this study).

5. Discussion

5.1 Syn-collisional granitoids of EKOB

The ophiolites from the Anyemaqen suture zone were considered as fragments of the Paleo-Tethys Ocean crust (Bian et al., 2004; Konstantinovskaia et al., 2003; Sigoyer et al., 2014; Yang et al., 1996, 2009). The Anyemaqen Ocean, which is a part of Paleo-Tethys Ocean (Fig. 12a), was probably opened at or before the Early Carboniferous according to the zircon U-Pb analyses of gabbros (332.8±3.1 Ma; Liu et al., 2011) and basalts (308.0±4.9 Ma; Yang et al., 2009). The Anyamaqen Ocean may have been closed at the Early-Triassic according to the Hongshuichuan formation which is composed of shallow marine facies and fluvial facies strata. The angular unconformity between the Late-Triassic terrestrial Babaoshan formation and the underlying Early-Triassic shallow marine Naochangjian formation also indicate the onset of the collision at the Early-Triassic (Li et al. 2012; Yan et al., 2008).

The late Permian molasses and the absence of the Permian magmatic rocks (1:250000 Donggi Conag Lake geological map sheet; China University of Geoscience, Wuhan, 2003) indicate a continental uplift event during that time. The absence of late Middle-Triassic to early Late-Triassic strata in East Kunlun demonstrates that partial small-scale collision transferred into comprehensive large-scale collision during this stage. Hence, we can infer that the Dulan batholith (~235Ma-240Ma, also 220Ma)

reported here are syn-collisional granitoids in response to the collision of the Songpan-Garze terrane and Qaidam terrane (Fig. 12b).

5.2 Source and melting mechanism of the syn-collisional granitoids

The petrogenesis of the Triassic granitoids of the EKOB is controversial. Xia et al. (2014) interpreted the Xiao-Nuomuhong pluton (~222 Ma; middle part of the EKOB) as the mixture of thickened lower crust derived melts and lithospheric mantle derived melts in response to slab breakoff of the Paleo-Tethys seafloor. Chen et al. (2015a) also considered the granodiorites from Qimantage area (240-238 Ma; west of the EKOB) as a result of slab breakoff during the transition from subduction to collision. Luo et al. (2014) proposed that the Xiangride intrusion (~223 Ma) was originated from ancient lower crust resulted from basaltic magma underplating after post-collisional lithosphere delamination although the mechanism of delamination is unclear (Lee et al., 2015; Sacks and Secor, 1990).

Bowen (1928) proposed that granite can also be products of crystallization differentiation from mantle-derived basaltic magma under high temperature (900~1000°C) and water-undersaturated conditions. The Hf isotopic data of Dulan batholith ($\varepsilon_{Hf}(t)$ = – 0.83 to + 3.68) and other East Kunlun Triassic granitoids (Figs 10c, d; Ding et al., 2015; Huang et al., 2014; Xia et al., 2015; Zhang et al., 2015) are indicative of significant mantle contribution. Figure 8 shows that the Nb* and Ta* values of the Dulan batholith are obviously lower than the values of the peralkaline rhyolites resulting from protracted fractional crystallization of mantle-derived alkali basaltic melts (Shao et al., 2015). Since the $D_{Nb} \approx D_{Th} < D_{Ta} \approx D_{U}$ during magma evolution (Niu and Batiza, 1997), the lower Nb/Th (or Nb*) and Ta/U (or Ta*) feature of the granitoids (which is identical to the BCC, also see Fig. 7b) must have been inherited from sources or source histories. Therefore, the Dulan batholith cannot be

products of mantle-derived basaltic magma. The bulk-rock Nd isotopic feature ($\varepsilon_{Nd}(t)$ = – 6.40 to – 5.10) of the Dulan batholith suggests that there must be contributions of continental crustal materials. Because the pre-existing old crustal materials have rather lower Nd and Hf isotopes (e.g., RSX12-12，$\varepsilon_{Nd}(t)$ = -17.0 and $\varepsilon_{Hf}(t)$ = -15.5, t = 235 Ma; Fig. 11b; Appendix Table 3), this mature crustal materials cannot be the main sources of the syn-collisional Triassic granitoids.

Partial melting of the basaltic oceanic crust can produce large volumes of andesitic plutons with mantle isotope signature (Chen et al., 2015b, 2016; Huang et al., 2014; Mo et al., 2008; Niu et al., 2013; Zhang et al., 2015). Here we infer that the underthrust Paleo-Tethys oceanic crust may be the most probable candidate for the syn-collisional andesitic magmatism of the EKOB. Simple Sr-Nd-Hf isotopes mass balance calculation shows that melting of source rocks equivalent to ~ 85% Paleo-Tethys MORB and ~15% mature crustal material (Proterozoic gneiss, RSX12-12) can explain the petrogenesis of the Dulan batholith (Fig. 11). For the mechanism and conditions of the partial melting of the ocean crust and sediments, Mo et al. (2008) proposed that the ocean crust and sediments can melt under amphibolite face conditions (also see Niu et al., 2013). The underthrusting cold Anyemaqen Ocean crust evolves along a high T/P geothermal path and has longer time to absorb heat from the prior hot active continental margin. The highly hydrated ocean crust (along with minor terrestrial sediments) begins to melt when it reaches the hydrous basaltic solidus under amphibolite conditions (see details in Mo et al., 2008; Niu et al., 2013).

The origin of MMEs in granitoids has been the subject of debate (e.g., Barbarin, 2005; Chappell, 1996; Chen et al., 2015b; Dahlquis, 2002; Dodge and Kistler, 1990; Niu et al., 2013), but Chen et al. (2015b, 2016) demonstrated that the coeval MMEs in the North Qilian Orogen (~430 Ma) are most consistent with early stage cumulate of

mafic minerals of the same magmatic system, which argues against the interpretations of mantle melt origin (e.g., Barbarin, 2005; Chen et al., 2009) and the restite model (e.g., Chappell, 1996; Chen et al., 1989). The Nb* and Ta* of the MMEs (except YDE12-05) are higher than the host granitoids which have similar values to the bulk continental crust (Fig. 8). This can be explained by the high partition coefficients of Nb (*vs.* Th) and Ta (*vs.* U) in amphiboles and Ti–Fe oxides because the MMEs represent accumulation of more mafic compositions dominated by amphiboles. Here we also consider the coeval MMEs are early liquidus mineral cumulate as they have the same mineralogy (but more mafic mineral, e.g., Amp and Bi), age and indistinguishable Sr-Nd-Hf isotope compositions as the host granitoids.

5.3 Quantitative modeling of our interpretation

We have done simple batch melting calculations (Fig. 13) with several reasonable assumptions to illustrate that partial melting under amphibolite face conditions: (1) the protolith is ~85% MORB and ~15% mature crustal material indicated by Sr-Nd-Hf isotopes discussed above; (2) the composition of the MORB is a combined "75% N-MORB and 25% E-MORB" based on the fact that about 75% of MORB with $[La/Sm]_N < 1$ and 25% of MORB with $[La/Sm]_N > 1$(Niu and O'Hara, 2003); (3) the mature crustal material is represented by the average composition of global subducted sediments (i.e., GLOSS; Plank and Langmuir, 1998); (4) the simplified mineral modes of the protolith are 66.4 wt. % hornblende, 4.4 wt. % ilmenite and 29.2 wt. % plagioclase (Niu and Lesher, 1991); (5) the mineral/melt partition coefficients (*Kd*) used are from the Geochemical Earth Reference Model (http://earthref.org/KDD/ and cf., Niu and O'Hara, 2009).

Figure 13 shows 5%, 10%, 20% and 30% batch melting of the chosen protolith. The model abundances of Th, Nb, U, Ta, Pb and LREEs match the Dulan batholith

and bulk continental crust compositions reasonably well. The negative anomalies of Nb and Ta (*vs.* Th, U and La) are produced with amphibole and ilmenite as residual phases. The calculated HREEs are higher than Dulan batholith and BCC. The HREEs contents will be lowered after crystallization of mafic minerals dominated by amphibolite and minor biotite as indicated by the REE patterns of the MMEs (Fig. 7). The Nb/Th and Ta/U ratios will be reduced accordingly against the protolith (Nb/Th = 4.78, Ta/U = 1.09), because the bulk partition coefficients $D_{Nb}>>D_{Th}$, $D_{Ta}>>D_{U}$ (D_{Nb} = 0.42, D_{Th} = 0.014, D_{Ta} = 0.383, D_{U} = 0.008; see above). As a result, the negative Nb* and Ta* anomalies are observed in Figure 8. In conclusion, 10% and 20% melting match the Dulan batholith and BCC better. The molding result provides circumstantial evidence in support of our interpretation, although this does not necessarily mean that the Dulan batholith is exactly produced by 10%-20% melting of the above assumed protolith.

5.4 Tectonic implications for the Qinling, Qilian and Kunlun orogenic belts

The Dulan batholith lies at the triple junction of the East Kunlun, West Qinling and Qilian orogenic belts (Fig. 1b). Jiang (1993) named Kunlun, Qinling and Dabie orogens (~4000km) the Central Orogenic Belt (COB) in order to emphasize their integrity and that they are located in the middle of China. The broadly-defined COB also contains the Qilian orogenic belt (Sun and Tian, 2001; Yin and Zhang, 1998; Zhang and Liu, 1998). The COB records both Proto-Tethys Ocean and Paleo-Tethys Ocean related subduction and collision events (Yin and Zhang, 1998; Zhang and Liu, 1998). The Tethys Ocean is thought to have been characterized by having multiple small continents as the result of breakup of the Gondwana supercontinent and accretion of the Eurasia continent (Bian et al., 2004; Dong et al., 2011;

Konstantinovskaia et al., 2003; Li et al., 2015; Pan et al., 1997; Sigoyer et al., 2014; Xu et al., 1998; Yang et al., 1996, 2009).

Yan et al. (2012) proposed that the West Qinling orogen is an accretionary wedge-shaped terrane and plunged into the Qilian and Kunlun orogenic belts during the Triassic (also see Fig. 8 of Xu et al., 2013). Considering: (1) the Triassic granitoids are widespread along the West Kunlun, East Kunlun and Qinling orogenic belts (e.g., Chen et al., 2013; Huang et al., 2014; Liu et al., 2003, 2004; Li et al., 2013; Luo et al., 2014; Xia, et al., 2014; Zhang et al., 2015); (2) the East Kunlun and West Qinling orogenic belts are separated by the northwest-southeast dextral strike-slip Wenquan fault; (3) the distribution of the Triassic plutons and volcanic rocks at the eastern end of the Kunlun orogen (e.g., Xiangride, Reshui and Yingdeer plutons; Fig. 2) and the western end of the Qinling orogen (e.g. Daheba, Tarxu and Xinghai plutons; 1: 1000 000 geological map of the Tibeten Plateau; Chengdu Institute of Geology and Mineral Resources; 2003) are parallel to the Wenquan fault, we infer that the Kunlun and Qinling orogens may actually be one single orogen offset later by the Wenquan fault system. Figure 12c shows this scenario. Under the near north-south compression (F_1) caused by the continental collision between the Qaidam terrane and Songpan-Garze terrane (Yin and Zhang, 1998), the Kunlun-Qinling orogen will yield near west-east tension and developed conjugated faults (*A* and *B*). The Wenquan fault was developed along shear plane *A* and this can also explain the distribution direction of the Triassic plutons and volcanic rocks. There are two groups of strike-slip fault (NNW and NE; Sun, 2014) which are consistent with these two sets of conjugate faults system in the East Kunlun and West Qinling. Kuhai-Shaishitang ophilite mélange zone is located in the Kunlun-Qinling conjunction area, northeast to the Dulan batholith. This zone developed all kinds of deformation, such as structural lens,

shear fold, boudin and mica fish (Sun, 2014). In conclusion, these geological observations support our inference.

As discussed in section 5.2, the petrogenesis of the Dulan batholith is consistent with an origin via partial melting of the last fragments of underthrusting Anyemaqen Ocean oceanic upper crust and the REE and trace element patterns of the Dulan batholith show remarkable similarity to the BCC (Fig. 7b). We thus suggest that the hypothesis of "continental collision zones as primary sites for net continental crust growth" (Niu et al., 2013) is applicable in the EKOB.

6. Conclusion

1. The ~240-220 Ma Dulan batholith of the EKOB is the product of syn-collisional magmatism during or shortly after the closure of the Anyemaqen Ocean.
2. The granitoids and MMEs have identical zircon U-Pb ages and also share the same mineralogy and indistinguishable Sr-Nd-Hf isotopic compositions, which support the recent model by Chen et al. (2015, 2016) that the MMEs represent earlier mafic cumulate of the same granitoid magmatic system.
3. The petrogenesis of the Dulan batholith of the EKOB is consistent with an origin via partial melting of the last fragments of underthrusting Anyemaqen Ocean oceanic upper crust under amphibolite facies conditions. Simple Sr-Nd-Hf isotopes mass balance calculations show that ~ 85% Paleo Tethys Oceanic MORB and ~15% continental material (Proterozoic gneiss) contribute to the source of the magmatism.
4. The Dulan batholith shows close compositional similarities to the bulk continental curst and has inherited mantle isotopic signatures. We demonstrate that the

hypothesis "continental collision zones are primary sites for net continental crust growth" applies in the EKOB.

Acknowledgements

We thank Wenli Sun and Yuxin Ma, Yan Hu, Guorui Zhang for field operation and Yu Zhang, Pu Sun, Huixia Cui, Lei Ye, Jinju Liu, Yan Hu, Zhenxing Hu , Jiyong Li for sample preparation. We thank Li Su, Hong Qin, Jinlong Ma, Xirong Liang for laboratory assistance in geochemistry and isotope analysis. We appreciate two anonymous reviewers for constructive comments and Editor Sun-Lin Chung for handing this manuscript. This work was supported by grants from National Natural Science Foundation of China (41130314, 41630968), Qingdao National Laboratory for Marine Sciences and Technology (2015ASKJ03) and the NSFC-Shandong Joint Fund for Marine Science Research Centers (U1606401), Chinese Academy of Sciences (Y42217101L).

References

Andersen, T., 2002. Correction of common lead in U-Pb analyses that do not report ^{204}Pb. *Chemical Geology* **192**, 59-79.

Ba., J., Gong, S., Liao, F., Zhang, L., 2012. Re-determining the intrusion age for the protolith of the Mohe gneiss in the Quanji Massif. *Geological Science and Technology Information* **31**, 98-101. (in Chinese with English abstract)

Barbarin, B., 2005. Mafic magmatic enclaves and mafic rocks associated with some granitoids of the central Sierra Nevada batholith, California: nature, origin, and relations with the hosts. *Lithos* **80**, 155-177.

Bian, Q., Li, D., Pospelov, I., Yin, L., Li, H., Zhao, D., Chang, C., Luo, X., Gao, S., Astrakhantsev, O., Chamov, N., 2004. Age, geochemistry and tectonic setting of Buqingshan ophiolites, North Qinghai-Tibet Plateau. *Journal of Asian Earth Science* **23**, 577-596.

Bowen, N. L., 1928. The Evolution of the Igneous Rocks. Princeton University Press, Pinceton, New Jersey, p332.

Chappell, B.W., 1996. Magma mixing and the production of compositional variation within granite suites: evidence from the granites of southeastern Australia. *Journal of Petrology* **37**, 449-470.

Chauvel, C., Lewin, E., Carpentier, M., Arndt, N.T., Marini, J.C., 2008. Role of recycled oceanic basalt and sediment in generating the Hf–Nd mantle array. *Nature Geoscience* **1**:64-67.

Chen, G., Pei, X., Li, R., Li, Z., Pei, L., Liu, Z., Chen, Y., Liu, C., 2013. Late Triassic magma mixing in the East Kunlun orogenic belt: A case study of Helegang Xilikete granodiorites. *Geology in China* **40**,1044-1065. (in Chinese with English abstract)

Chen, B., Chen, Z., Jahn, B., 2009. Origin of mafic enclaves from the Taihang Mesozoic orogeny, north China craton. *Lithos* **110**, 343-358.

Chen, J., Wang, B., Li, B., Zhang, Z., Qiao, B., Jin, T., 2015a. U–Pb ages, geochemistry, and Sr–Nd–Pb isotopic compositions of Middle Triassic granodiorites from the Kaimuqi area, East Kunlun, Northwest China: implications for slab breakoff. *International Geology Review* **57**, 257-270.

Chen, S., Niu, Y., Sun, W., Zhang, Y., Li, J., Guo, P., Sun, P., 2015b. On the origin of mafic magmatic enclaves (MMEs) in syn-collisional granitoids: evidence from the Baojishan pluton in the North Qilian Orogen, China. *Mineralogy and Petrology* **109**, 577-596.

Chen, S., Niu, Y., Li, J., Sun, W., Zhang, Y., Hu Y., Shao, F., 2016. Syncollisional adakitic granodiorites formed by fractional crystallization: insights from their enclosed mafic magmatiuc enclaves (MMEs) in the Qumushan pluton, North Qilian Orogen at the northern margin of the Tibetan Plateau. *Lithos* **248/251**, 455-468.

Chen, Y., Price, R.C., White, A.J.R., Chappell, B.W., 1989. Inclusions in three S-type granites from southeastern Australia. *Journal of Petrology 30*, 1181-1218.

Dahlquis, J.A., 2002. Mafic microgranular enclaves: early segregation from metaluminous magma (Sierra de Chepes), Pampean Ranges, NW Argentina. *Journal of South American Earth Sciences* **15**, 643-655.

Dai, J., Wang, C., Hourigan, J., Santosh, M., 2013. Multi-stage tectono-magmatic events of the Eastern Kunlun Range, northern Tibet: Insights from U–Pb geochronology and (U–Th)/He thermochronology. *Tectonophysics* **599**, 97-106.

Dai, J., Wang, C., Zhu, D., Li, Y., Zhong, H., Ge, Y., 2015. Multi-stage volcanic activities and geodynamic evolution of the Lhasa terrane during the Cretaceous: Insights from the Xigaze forearc basin. *Lithos* **218-219**, 127-140.

Ding, S., Huang, H., Niu, Y., Zhao, Z., Yu, X., Mo, X., 2011. Geochemistry, geochronology and petrogenesis of East Kunlun high Nb-Ta rhyolites. *Acta Petrologica Sinica* **27**, 3603-3614 (in Chinese with English abstract).

Ding, Q., Liu, F., Yan, W., 2015. Zircon U–Pb geochronology and Hf isotopic constraints on the petrogenesis of Early Triassic granites in the Wulonggou area of the Eastern Kunlun Orogen, Northwest China. *International Geology Review* **57**, 1735-1754.

Dodge F.C.W., Kistler, R.W., 1990. Some additional observations on inclusions in the granitic rocks of the Sierra Nevada. *Journal of Geophysical Research* **95**, 17841-17848.

Dong, Y., Zhang, G., Neubauer, F., Liu, X., Genser, J., Hauzenberger, C., 2011. Tectonic evolution of the Qinling orogen, China: Review and synthesis. *Journal of Asian Earth Science* **41**, 213-237.

Duretz, T., Gerya, T.V., May, D.A., 2011. Numerical modelling of spontaneous slab breakoff and subsequent topographic response. *Tectonophysics* **502**, 244-256.

Feng, S., Zhao, K., Ling, H., Chen, P., Chen, W., Sun, T., Jiang, S., Wei, P., 2014. Geochronology, elemental and Nd–Hf isotopic geochemistry of Devonian A-type granites in central Jiangxi, South China: Constraints on petrogenesis and post-collisional extension of the Wuyi-Yunkai orogeny. *Lithos* **206-207**, 1-18.

Gong, S., Chen, N., Wang, Q., Kusky, T. M., Wang, L., Zhang, L., Ba, J., Liao, F., 2012. Early Paleoproterozoic magmatism in the Quanji Massif, northeastern tectonic significance: LA-ICPMS U-Pb zircon geochronology and geochemistry. *Gondwana Reasearch* **21**, 152-166.

Guo, Z., Deng, J., Xu, Z., Mo, X., Luo, Z., 1998. Late Paleozoic-Mesozoic intracontinental orogenic process and intermediate-acidic igneous rocks from the eastern Kunlun mountains of notrthwestern China. *Geoscience* **12**, 344-352. (in Chinese with English abstract)

Hao, G., Lu, S., Wang, H., 2004. The Pre-Devonian tectonic framework in the northern margin of Qaidam basin and geological evolution of Olongbuluck palaeo-block. *Earth Science Frontiers* **11**, 115-122. (in Chinese with English abstract)

Hao, M., Ferymueller, J. T., Wang, Q., Cui, D., Qin, S., 2016. Vertical crustal movement around the southeastern Tibetan Plateau constrained by GPS and GRACE data. *Earth and Planetary Science Letters* **437**, 1-8.

He, S., Kapp, P., DeCelles, P. G., Gehrels, G. E., Heizler, M., 2007. Cretaceous-Tertiary geology of the Gangdese Arc in the Linzhou area, southern Tibet. *Tectonophysics* **433**, 15-37.

Hu, Y., Niu, Y., Li, J., Ye, L., Kong, J., Chen, S., Zhang, Y., Zhang, G., 2015. Petrogenesis and tectonic significance of the Late Triassic mafic dikes and felsic volcanic rocks in the East Kunlun Orogenic Belt, Northern Tibet Plateau. *Lithos*, **245**, 205-222.

Huang, H., Niu, Y., Nowell, G., Zhao, z., Yu, X., Zhu, D., Mo, X., Ding, S., 2014. Geochemical constraints on the petrogenesis of granitoids in the East Kunlun Orogenic blet, northern Tibetan Plateau: implications for the continental crust growth through syncollisional felsic magmatism. *Chemical Geology* **370**, 1-18.

Huang, H., Niu, Y., Nowell, G., Zhao, Z., Yu, X., Mo, X., Ding, S., 2015. The nature and history of the Qilian Block in the context of the development of the Greater Tibetan Plateau. *Gondwana Research* **28**, 209-224.

Hoskin, P. W. O., Schaltegger, U., 2003.The composition of zircon and igneous and metamorphic petrogenesis. *Reviews in mineralogy and geochemistry* **53**, 27-55.

Ji, W., Wu, F., Chung, S., Li, J., Liu, C., 2009. Zircon U–Pb chronology and Hf isotopic constraints on the petrogenesis of Gangdese batholiths, southern Tibet. *Chemical Geology* **262**, 229-245.

Jiang, C., 1993. The major geological and structural characters of Certral Orogenic Belt. *Geology Research* **27**, 107-108. (in Chinese)

Kang, Z., Xu, J., Wang, B., Dong, Y., Wang, S., Chen, J., 2009. Geochemistry of Cretaceous volcanic rocks of Duoni Formation in northern Lhasa block: discussion

of tectonic setting. *Earth Science-Journal of China University of Geosciences* 34, 89-104.

Konstantinovskaia, E. A., Brunel, M., Malavieille, J., 2003. Discovery of the Paleo-Tethys residual peridotites along the Anyemaqen-KunLun suture zone (North Tibet). *Comptes Rendus Geoscience* **335**, 709-719.

Lee, H., Chung, S., Lo, C., Ji, J., Lee, T., Qian, Q., Zhang, Q., 2009. Eocene Neotethyan slab breakoff in southern Tibet inferred from the Linzizong volcanic record. *Tectonophysics* **477**, 20-35.

Lee, C. T. A., Anderson, D. L., 2015. Continental crust formation at arcs, the arclogite "delamination" cycle, and one origin for fertile melting anomalies in the mantle. *Science Bulletin* **60**, 1141-1156.

Li, R., Pei, X., Li, Z., Liu, Z., Chen, G., Chen, Y., Wei, F., Gao, J., Liu, C., Pei, L., 2012. Geological characteristics of Late Paleozoic-Mesozoic unconformities and their response to some significant tectonic events in eastern part of Eastern Kunlun. *Earth Science Frontiers* **19**, 244-254.

Li, X., Mo, X., Huang, X., Dong, G., Yu, X., Luo, M., Liu, Y., 2015. U–Pb zircon geochronology, geochemical and Sr–Nd–Hf isotopic compositions of the Early Indosinian Tongren Pluton in West Qinling: Petrogenesis and geodynamic implications. *Journal of Asian Earth Science* **97**, 38-50.

Li, X., Qi, C., Liu, Y., Liang, X., Tu, X., Xie, L., Yang, Y., 2005. Rapid separation of Hf from rock samples for isotope analysis by MC-ICPMS: A modified single-column extraction chromatography methord. *Geochimica* **34**, 109-114.

Liang, S., Gan, W., Shen, C., Xiao, G., Liu, J., Chen, W., Ding, X., Zhou, D., 2013. Three-dimensional velocity field of present-day crustal motion of the Tibetan Plateau derived from GPS measurements, *Journal of Geophysical Research: Solid Earth* **118**, 5722-5732.

Liu, C., Mo, X., Luo, Z., Yu, X., 2003. Pb-Sr-Nd-O isotope characteristics of granitoids in east Kunlun orogenic belt. *Acta Geoscientica Sinica* **24**, 584-588. (in Chinese with English abstract)

Liu, C., Mo, X., Luo, Z., Yu, X., 2004. Mixing events between the crust and mantle derived magmas in eastern Kunlun: evidence from zircon SHRIMP chronology. *Chinese Science Bulletin* **49**, 828-834. (in Chinese)

Liu, Y., Mo, X., Yu, X., Zhang, X., Xu, G., 2006., Zircon shrimp U-Pb dating of the Jingren granite, Yemaquan region of the east Kunlun and its geological significance. *Acta Petrologica Sinica* **22**, 2457-2463. (in Chinese with English abstract)

Liu, Y., Hu, Z., Gao, S., Günther, D., Xu, J., Gao, C., Chen, H., 2008. In situ analysis of major and trace elements of anhydrous minerals by LA-ICP-MS without applying an internal standard. *Chemical Geology* **257**, 34-43.

Liu, Y., Gao, S., Hu, Z., Gao, C., Zong, K.,Wang, D., 2010. Continental and oceanic crust recycling-induced melt- peridotite interactions in the trans-North China Orogen: U-Pb dating, Hf isotopes and trace elements in zircons from mantle xenoliths. *Journal of Petrology* **51**, 537-571.

Liu, Z., Pei, X., Li, R., Li, Z., Zhang, X., Liu, Z., Chen, G., Chen, Y., Ding, P., Guo, X., 2011. La-ICP-MS zircon U-Pb dating of two suits of ophiolites at the Buqingshan area of the A'nyemaqen Orogenic belt in the Southern Margin of the East Kunlun and its tectonic implication. *Acta Geologica Sinica* **85**, 185-194.

Liu, Z., Jiang, Y., Jia, R., Zhao, P., Zhou, Q., 2015. Origin of Late Triassic high-K calc-alkaline granitoids and their potassic microgranular enclaves from the western Tibet Plateau, northwest China: Implications for Paleo-Tethys evolution. *Gondwana Research* **27**, 326-341.

Ludwig, K. R., 2003. Isoplot 3.00: A Geochronological Toolkit for Microsoft Excel. Berkeley Geochronology Center, Berkeley, CA.

Luo, M., Mo, X., Yu, X., Li, X., Huang, X., Yu, J., 2014. Zircon LA-ICP-MS U-Pb dating, petrogenesis and tectonic implication of the Late Triassic granites from Xiangride area, East Kunlun. *Acta Petrologica Sinica* **30**, 3229-3241. (in Chinese with English abstract)

Luo, Z., Ke, S., Cao, Y., 2002. Late Indosinian mantle-derived magmatism in the East Kunlun. *Geological Bulletin of China* **21**, 291-297. (in Chinese with English abstract)

Mo, X., Dong, G., Zhao, Z., Guo, T., Wang, L., Chen, T., 2005. Timing of magma mixing in Gangdise magmatic belt during the India–Asia collision: zircon SHIRMP U–Pb dating. *Acta Geologica Sinica* **79**, 66-76.

Mo, X., Hou, Z., Niu, Y., Dong, G., Qu, X., Zhao, Z., Yang, Z., 2007. Mantle contributions to crustal thickening during continental collision: Evidence from Cenozoic igneous rocks in southern Tibet. *Lithos* **96**, 225-242.

Mo, X., Luo, Z., Deng, J., Yu, X., Liu, C., Tan, H., Yuan, W., Liu, Y., 2007. Granitoids and crust growth in the East-Kunlun Orogenic Belt. *Geological Journal of China Universities* **13**, 403-414. (in Chinese with English abstract)

Mo, X., Niu, Y., Dong, G., Zhao, Z., Hou, Z., Zhou, S., Ke, S., 2008. Contribution of syncollisional felsic magmatism to continental crust growth: a case study of the Paleocene Linzizong Volcanic Succession in southern Tibet. *Chemical Geology* **250**, 49-67.

Mo, X., Zhao, Z., Deng, J., Dong, G., Zhou, S., Guo, T., Zhang, S., Wang, L., 2003. Response of volcanism to the India–Asia collision. *Earth Science Frontier* **10**, 135-148 (in Chinese with English abstract).

Niu, Y., Lesher, C.M., 1991. Hydrothermal alteration of mafic metavolcanic rocks and genesis of Fe-Zn-Cu sulfide deposits, Stone Hill district, Alabama. *Economic Geology* **86**, 983-1001.

Niu, Y., & Batiza, R., 1997. Extreme mantle source heterogeneities beneath the northern East Pacific Rise – Trace element evidence from near-ridge seamounts. Proceedings of 30th ICG, Volume 15, 109-120.

Niu, Y., Hékinian, R., 1997. Basaltic liquids and harzburgitic residues in the Garrett Transform: A case study at fast-spreading ridges. *Earth and Planetary Science Letters* **146**, 243-258.

Niu, Y., Collerson, K.D., Batiza, R., Wendt, J.I. and Regelous, M., 1999. The origin of E-Type MORB at ridges far from mantle plumes: The East Pacific Rise at 11°20'. *Journal of Geophysical Research* **104**, 7067-7087.

Niu, Y., O'Hara, M.J., 2003. The origin of ocean island basalts (OIB): A new perspective from petrology, geochemistry and mineral physics considerations. *Journal of Geophysical Research* **108**, ECV5 1-19.

Niu, Y., O'Hara, M.J., 2009. MORB mantle hosts the missing Eu (Sr, Nb, Ta and Ti) in the continental crust: new perspectives on crustal growth, crust–mantle differentiation and chemical structure of oceanic upper mantle. *Lithos* **112**, 1-17.

Niu, Y., Zhao, Z., Zhu, D., Mo, X., 2013. Continental collision zones are primary sites for net continental crust growth–a testable hypothesis. *Earth Science Review* **127**, 96-110.

Pan, G., Chen, Z., Li, X., 1997. Geological Tectonic Evolution in the Eastern Tethys. Beijing: Geological Publishing House, 1-217. (in Chinese)

Plank, T., Langmuir, C. H., 1998. The chemical composition of subducting sediment and its consequences for the crust and mantle. *Chemical Geology* **145**, 325-394.

Ravikant, V., Wu, F., Ji, W., 2009. Zircon U–Pb and Hf isotopic constraints on petrogenesis of the Cretaceous-Tertiary granites in eastern Karakoram and Ladakh, India. *Lithos* **110**, 153-166.

Rudnick, R.L., Gao, S., 2003. Composition of the continental crust. In: Holland, H.D., Turekian, K.K. (Eds.), Treatise on Geochemistry 3. Elsevier-Pergamon, Oxford, pp. 1-64.

Shao, F., Niu, Y., Marcel, R., Zhu, D., 2015. Petrogenesis of peralkaline rhyoliths in an intro-plate setting: Glass House Mountains, southeast Queensland, Australia. *Lithos* **216-217**, 196-210.

Sigoyer, J. D., Vanderhaeghe, O., Duchêne, S., Billerot, A., 2014. Generation and emplacement of Triassic granitoids within the Songpan Ganze accretionary-orogenic wedge in a context of slab retreat accommodated by tear faulting, Eastern Tibetan plateau, China. *Journal of Asia Earth Science* **88**, 192-216.

Sun, G., Hu, X., Zhu, D., Hong, W., Wang, J., Wang, Q., 2015. Thickened juvenile lower crust-derived ~90 Ma adakitic rocks in the central Lhasa terrane, Tibet. *Lithos* 224-225, 225-239.

Sun, S.S., McDonough, W.F., 1989. Chemical and isotopic systematics in ocean basalt: implications for mantle composition and processes. Geological Society 42. Special Publications, London, pp. 313-345.

Sun, Y., Tian Q., 2001. Features of junction of Qinling, Qilian and Kunlun orogenic belts. *Geology of Qinghai* **1**, 16-20.

Sun, Y., 2014. Gonghe aolacogen and conjugate and transfer between the west Qinling and east Kunlun orogens. Northwest University, Xi'an.

Sacks, P.E., Secor, D.T., 1990. Delamination in collisional orogens. *Geology* **18**, 999-1002.

Song, S., Niu, Y., Su, L., Xia, X., 2013. Tectonics of the North Qilian orogen, NW China. *Gondwana Research* **23**, 1378-1401.

Song, S., Zhang, L., Niu, Y., Wei, C., Liou, J.G., Shu, M., 2007. Eclogite and carpholite-bearing metasedimentary rocks in the North Qilian suture zone, NW China: implications for Early Palaeozoic cold oceanic subduction and water transport into mantle. *Journal of Metamorphic Geology* **25**, 547-563.

Taylor, S.R., 1967. The origin and growth of continents. *Tectonophysics* 4, 17-34.

Wan, Y., Liu, D., Dong, C., Yin, X., 2011. SHRIMP zircon dating of meta-sedimentary rock from the Qinling Group in the north of Xixia, North Qinling Orogenic Belt: Constraints on complex histories of source region and timing of depositionand metamorphism. *Acta Petrologica Sinica* **27**, 1172-1178. (in Chinese with English abstract)

Wang, M., Song, S., Niu, Y., Su, L., 2014. Post-collisional magmatism: Consequences of UHPM terrane exhumation and orogen collapse, N. Qaidam UHPM belt, NW China. *Lithos* 210-211, 181-198.

Wen, D., Liu, D., Chung, S., Chu, M., Ji, J., Zhang, Q., Song, B., Lee, T., Yeh, M., Lo, C., 2008. Zircon SHRIMP U–Pb ages of the Gangdese batholith and implications for Neotethyan subduction in southern Tibet. *Chemical Geology* **252**,191-201.

Wiedenbeck, M., Alle, P., Corfu, F., Grian, W. L., Meier, M., Oberli, F., Quadt, A., Roddick, J. C. and Spiegel, W., 1995. Three natural zircon standards for U-Th-Pb, Lu-Hf, trace element and REE analyses. *Geostandards Newsletter* 19, 1-23.

Xia, R., Wang, C., Deng, J.,Carrancz, E. J.M., Li, W., Qing, M., 2014. Crustal thickening prior to 220 Ma in the East Kunlun Orogenic Belt: Insights from the Late Triassic granitoids in the Xiao-Nuomuhong pluton. *Journal of Asian Earth Science* 93, 193-210.

Xia, R., Wang, C., Qing, M., Li, W., Carranza, E. J. M., Guo, X., Ge, L., Zeng, G., 2015. Zircon U–Pb dating, geochemistry and Sr–Nd–Pb–Hf–O isotopes for the Nan'getan granodiorites and mafic microgranular enclaves in the East Kunlun Orogen: Record of closure of the Paleo-Tethys. *Lithos* **234-235**, 47-60.

Xu, J., Yu, X., Li, X., Han, Y., Shen, J., Zhang, B., 1998. Discovery of the highly depleted N-MORB-type volcanic rocks: new evidence for the Mianlue paleo-ocean. *Chinese Science Bulletin* **43**, 510-514.

Xu, J., Castillo, P. R., 2004. Geochemical and Nd–Pb isotopic characteristics of the Tethyan asthenosphere: implications for the origin of the Indian Ocean mantle domain. *Tectonophysics* **393**, 9-27.

Xu, Y., Du, Y., Cawood, P.A., Guo, H., Huang, Y., An, Z., 2010. Detrital zircon record of continental collision: Assembly of the Qilian Orogen, China. *Sedimentary Geology* **230,** 35-45.

Xu, Z., Yang, J., Li, H., Zhang, J., Wu, C., 2007. Orogenic Plateau: Terrane Amalgamation, Collision and Uplift in the Qinghai-Tibet Plateau. Beijing: Geological Publishing House, 1-458. (in Chinese with English abstract)

Xu, Z., Yang, J., Li, W., Li, H., Cai, H., Yan, Z., Ma, C., 2013. Paleo-Tethys system and accretionary orogen in the Tibet Plateau. *Acta Petrologica Sinica* **29**: 1847-1860.

Xue, H., Dong, S., Ma, F., 2010. Zircon U-Pb ages of volcanic bodies related with porphyritic Fe deposits in the Luzong and Ningwu basins, Middle and Lower Yangtze River Rearches, Central China. *Acta Petrologica Sinica* **26**, 2653-2664. (in Chinese with English abstract)

Yan, Z., Bian, Q., Korchagin, O. A., Pospelov, I. I., Li, J., Wang, Z., 2008. Provenance of Early Triassic Hongshuichuan Formation in the southern margin of the East Kunlun Mountains: Constrains from detrial framework, heavy mineral analysis and geochemistry. *Acta Petralogica Sinica* **24**, 1068-1078. (in Chinese with English abstract)

Yang, J., Robinson, P.T., Jiang, C., Xu, Z., 1996. Ophiolites of the Kunlun mountains, China and their tectonic implications. *Tectonophysics* **258**, 215-231.

Yan, Z., Wang, Z., Li, J., Xu, Z., Deng, J., 2012. Tectonic settings and accretionary orogenesis of the West Qinling Terrane, northeastern margin of the Tibet Plateau. *Acta Petrologica Sinica* **28**: 1808-1828.

Yang, J., Shi, R., Wu, C., Wang, X., Robinson, P.T., 2009. Dur'ngio ophiolite in east Kunlun, northeast Tibetan Plateau: Evidence for Paleo-Tethyan suture in northwest China. *Journal of Earth Science* **20**, 303-331.

Yang, H., Zhang, H., Luo, B., Xiong, Z., Guo, L., Pan, F., 2015. Early Paleozoic intrusive rocks from the eastern Qilian orogen, NE Tibetan Plateau: Petrogenesis and tectonic significance. *Lithos* **224-225**, 13-31.

Yin, H., Zhang, K., 1998. Evolution and characteristics of the central orogenic belt. Earth Science: *Journal of China University of Geosciences* **23**, 438-442. (in Chinese with English abstract)

Zhang, G., Liu, X., 1998. Some remarks on China central orogenic system. *Earth Science: Journal of China University of Geosciences* **23**, 443-448. (in Chinese with English abstract)

Zhang, Y., Niu, Y., Hu, Y., Liu, J., Ye, L., Kong, J., Duan, M., 2015. The syncollisional granitoid magmatism and continental crust growth in the West Kunlun Orogen, China – Evidence from geochronology and geochemistry of the Arkarz pluton. *Lithos* **262**, 107-119.

Zhu, D., Wang, Q., Zhao, Z. Chung, S., Wood, P., Niu, Y., Liu, S., Wu, F., Mo, X., 2015. Magmatic record of India-Asia collision. *Scientific Reports* **5**, 14289.

Zindler, A., Hart, S., 1986. Chemical geodynamics. *Earth and Planetary Science Letters* **14**:493-571.

Figure captions

Fig. 1 (a) Simplified map of the major tectonic units of the Greater Tibetan Plateau (after Mo et al., 2008; Niu et al., 2013). The plateau was amalgamated through a series of continental collision events progressively younger from northeast to southwest. (b) Schematic map showing that the East Kunlun Orogenic Belt (EKOB) lies nearby the triple junction of the East Kunlun, West Qinling and Qilian orogenic belts (after Yan et al., 2012). (c) Topographic image showing the sub-tectonic zones of the EKOB (from http://landsat.datamirror.csdb.cn). The thin lines in blue indicate suture zones as in (a). Blue circles are sample locations of previous studies (Chen et al., 2015a; Luo et al., 2014; Xia et al., 2014).

Fig. 2 Simplified geological map of the study area with sample locations indicated with yellow circles (the numbers next to the circles correspond to sequences numbers in Appendix Table 1), modified from Dulan Sheet of the 1: 250 000 geological map series (Tianjin Center of Geological Survey, 2003) and Donggi Conag Lake sheet (China University of Geoscience, Wuhan, 2003).

Fig. 3 (a) Field occurrences of granodiorite with mafic magmatic enclaves (MMEs) of varying size and sub-parallel distribution. (b) Photomicrograph under plane polarized light of the host granodiorite and MMEs with a gradational contact between the two as indicated by the light-blue dashed line. (c, d) Photomicrographs under crossed polarized light of representative granodiorite. Amphiboles in SJK12-02 are euhedral with simple twinning. Amp = amphibole, Bi = biotite, Kfs = K-feldspar, Mag = magnetite, Pl = plagioclase and Qz = quartz.

Fig. 4 (a-g) Panels of zircon U-Pb Concordia diagram. The zircon U-Pb age data indicate that the main parts of the Dulan batholith were emplaced at 240-235 Ma. (h) Zircon U-Pb ages of the granitic gneiss of the Paleoproterozoic basement. (i)

Cathodoluminescence (CL) images of zircons from representative host granitoid and MME samples. Yellow circles are the analyzed spots.

Fig. 5 (a) Total alkalis vs. Silica diagram to show the compositional variation of the Dulan batholith. (b) A/CNK vs. A/NK diagram. A/CNK = molar [Al_2O_3/(CaO + Na_2O+K_2O)]; A/NK = molar [Al_2O_3/(Na_2O+K_2O)].

Fig. 6 SiO_2 variation diagrams of major element oxides (wt. %). TiO_2, Al_2O_3, $Fe_2O_3^T$, MnO, MgO, CaO and P_2O_5 decrease with increasing SiO_2. K_2O increases with increasing SiO_2, while Na_2O shows no correlation.

Fig. 7 (a) Chondrite-normalized (Sun and McDonough, 1989) REE patterns for the granitoids and MMEs of the Dulan batholith. For comparison, the compositions of the Late Triassic rhyolites from this area are also showed (Hu et al., 2015). (b) Primitive mantle (Sun and McDonough, 1989) normalized multi-element diagram for average compositions of the host granitoids and MMEs. The bulk continental crust (BCC; Rudnick and Gao, 2003) is also plotted for comparison. The trace element composition of the Dulan batholith shows close similarities to the BBC.

Fig. 8 (a) Nb*-Ta* anomaly diagram (after Niu and Batiza, 1997; Niu et al., 1999). The Dulan batholith data plot close to the bulk continental crust (BCC; Rudnick and Gao, 2003), rather lower than those of mantle derived melts (peralkaline rhyolites from eastern Australia (see Shao et al., 2015). Average OIB, E-MORB, N-MORB (Niu and O'Hara; 2003), primitive mantle (PM; Sun and McDonough, 1989) and BCC compositions are plotted for comparison. (b). The Nb/Ta ratios (except YDE12-22) fall in the range between the chondrite (Nb/Ta = 17.57; Sun and Mcdonough, 1989) and BCC (Nb/Ta = 11.43).

Fig. 9 (a) The bulk-rock Rb-Sr pseudo-chron age (229 Ma) defined by all our granitoid samples is similar to the zircon U-Pb ages (~240-235 Ma). (b) Excluding the high Rb/Sr sample DLX12-07, the Rb-Sr pseudo-chron age (211 Ma) is also similar to the zircon U-Pb ages. (c) The Sm-Nd pseudo-chron age (271 Ma) also resemble the zircon U-Pb ages. (d) The Lu-Hf pseudo-chron age (424 Ma) is much older than the zircon U-Pb ages.

Fig. 10 (a-c) Bulk-rock ($^{87}Sr/^{86}Sr)_i$, $\varepsilon_{Hf}(t)$ and $\varepsilon_{Nd}(t)$ isotope data of the EKOB granitoids. For panels b and c, legend Dulan (red circle) represents both host rocks and the MMEs. The reference data about syn-collisional granitoids are from the North Qilian orogen (orange square, ~430 Ma, Chen et al., 2015a), West Kunlun orogen (blue diamond, ~225 Ma, Zhang et al., 2015) and East Kunlun orogen (green triangle, 250 Ma, Huang et al., 2014). These granitoid have similar Sr-Nd-Hf isotope features. (d) The $\varepsilon_{Hf}(t)$ characteristics of the Triassic granitoids of the Kunlun orogenic belt. Light blue diamonds (whole rock data, West Kunlun; Zhang et al., 2015); green triangles (whole rock data, East Kunlun; Huang et al., 2014); purple crosses and blue crosses (zircon data, East Kunlun; Ding et al., 2015; Xia et al., 2015).

Fig. 11 (a) The Sr-Nd-Hf isotopes for both granitoids and MMEs are indistinguishable and the source rocks can be modeled by mixing of ~ 85% Paleo Tethys Oceanic MORB and ~15% mature crustal material (Proterozoic gneiss). The endmember A is the mean value of the Paleo Tethys MORB (n=5; Sr = 333.8 ppm, Nd = 6.2 ppm, Hf = 1.31ppm, $(^{87}Sr/^{86}Sr)_i = 0.70599$, $(^{143}Nd/^{144}Nd)_i = 0.51250$, $\varepsilon_{Nd}(t) = 5.74$, $\varepsilon_{Hf}(t) = 10.41$) from the Jinshajiang suture (Xu and Castillo, 2004). The endmember B is a Proterozoic gneiss sample (RSX12-12) collected from the same region as the granitoids. (b) Although the Nd and Hf isotopes deviate from the mantle array and

seem to be “decoupled”, the Sr-Nd-Hf isotopes can be well modeled by mixing of the Paleo Tethys MORB and the old continental material in the study area.

Fig. 12 Cartoons showing (a) subduction of the Anyemaqen seafloor during the Carboniferous and Permian, (b) collision of the Qaidam terrane and Songpan-Garze terrane during the Triassic, and (c) development of conjugated faults (*A* and *B*) under the near north-south compression (F_1) in response to the continental collision, through which the Wenquan fault developed along an A-plane and offset the Kunlung-Qingling orogenic belts.

Fig. 13 Simple batch melting calculations showing the effectiveness of our interpretation on the petrogenesis of the syn-collisional granitoids of the EKOB. The source rocks are best molded by contributions of ~85% MORB (75% N-MORB and 25% E-MORB, Niu and O’Hara, 2003) and ~15% mature crustal materials (e.g., GLOSS; Plank and Langmuir, 1998) in terms of Sr-Nd-Hf isotopes. The simplified mineral modes are 66.4 wt. % hornblende, 4.4 wt. % ilmenite and 29.2 wt. % plagioclase (Niu and Lesher, 1991). The mineral partition coefficients are from the Geochemical Earth Reference Model (http://earthref.org/KDD/). All the data are normalized against average MORB with 75% N-MORB and 25% E-MORB (Niu and O’Hara, 2003). 10% and 20% batch melting of the assumed protolith reproduces the Dulan batholith compositions (EKOB) reasonably well except for the HREEs.

Figure 1

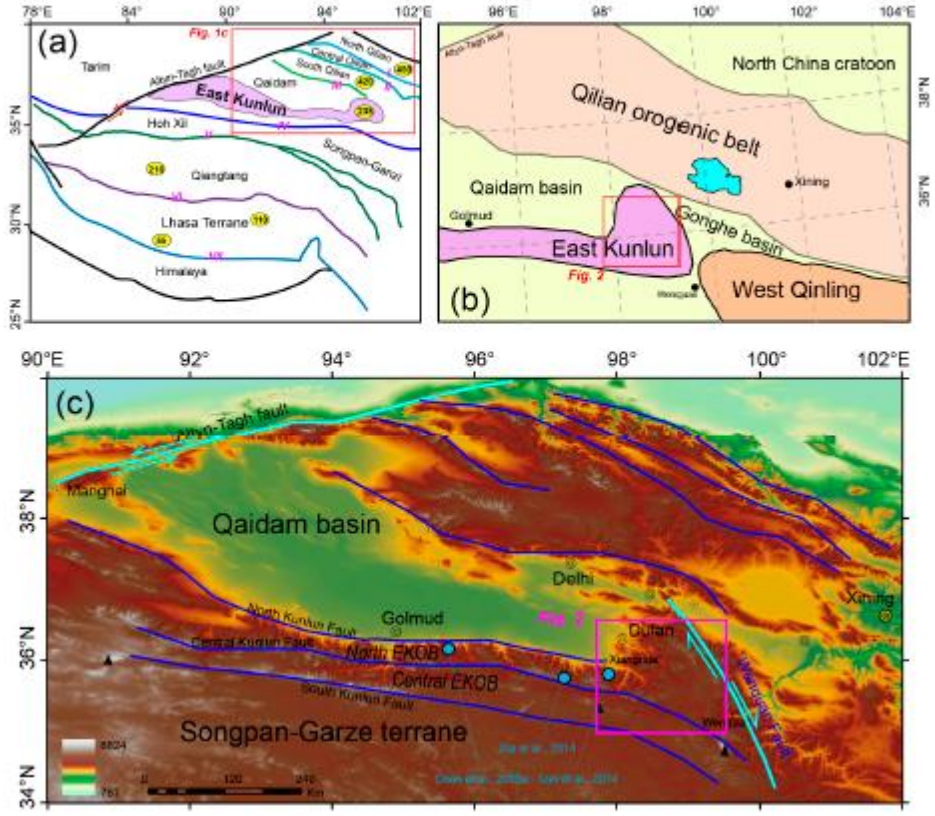

Figure 2

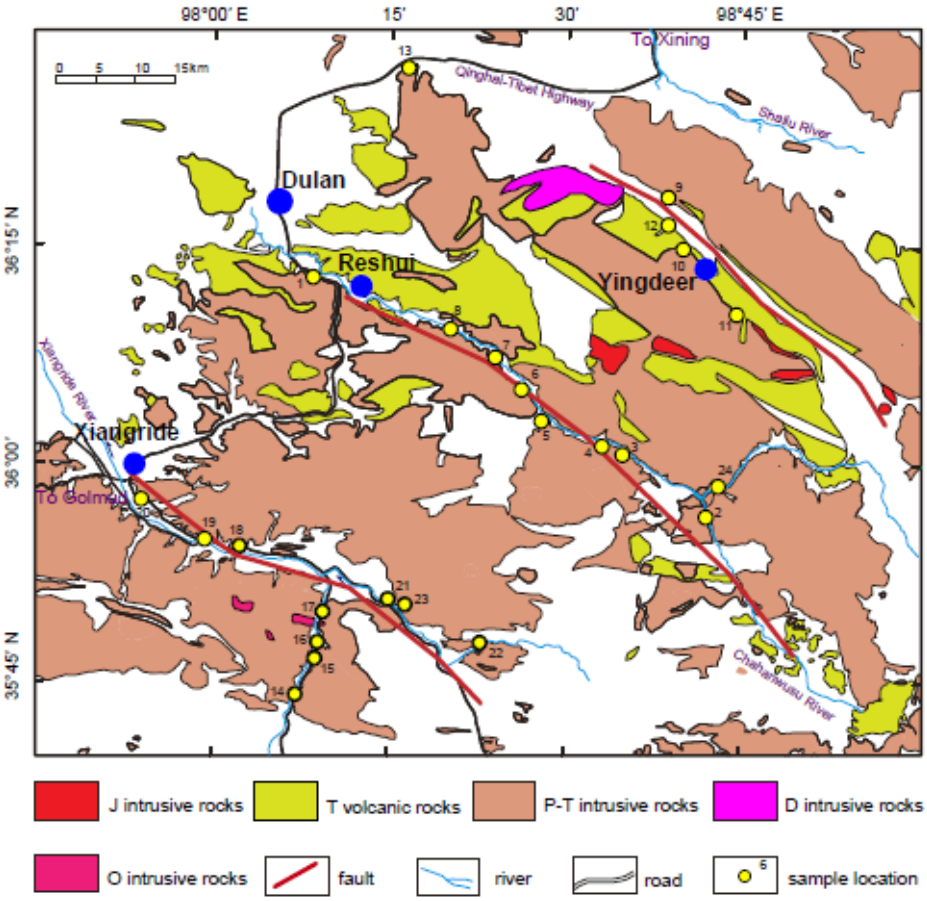

Figure 3

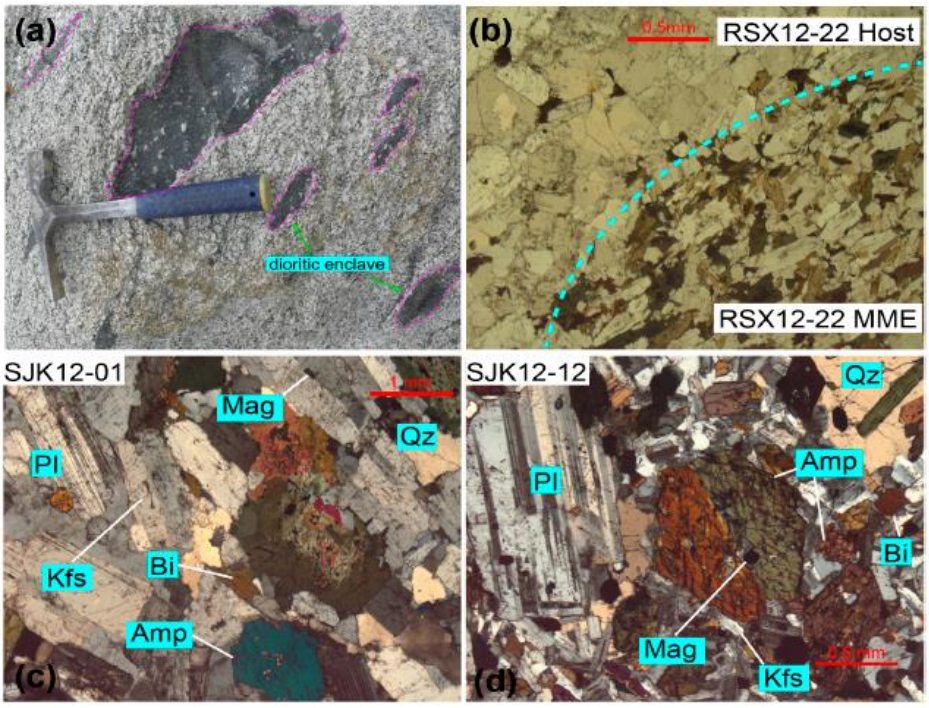

Figure 4

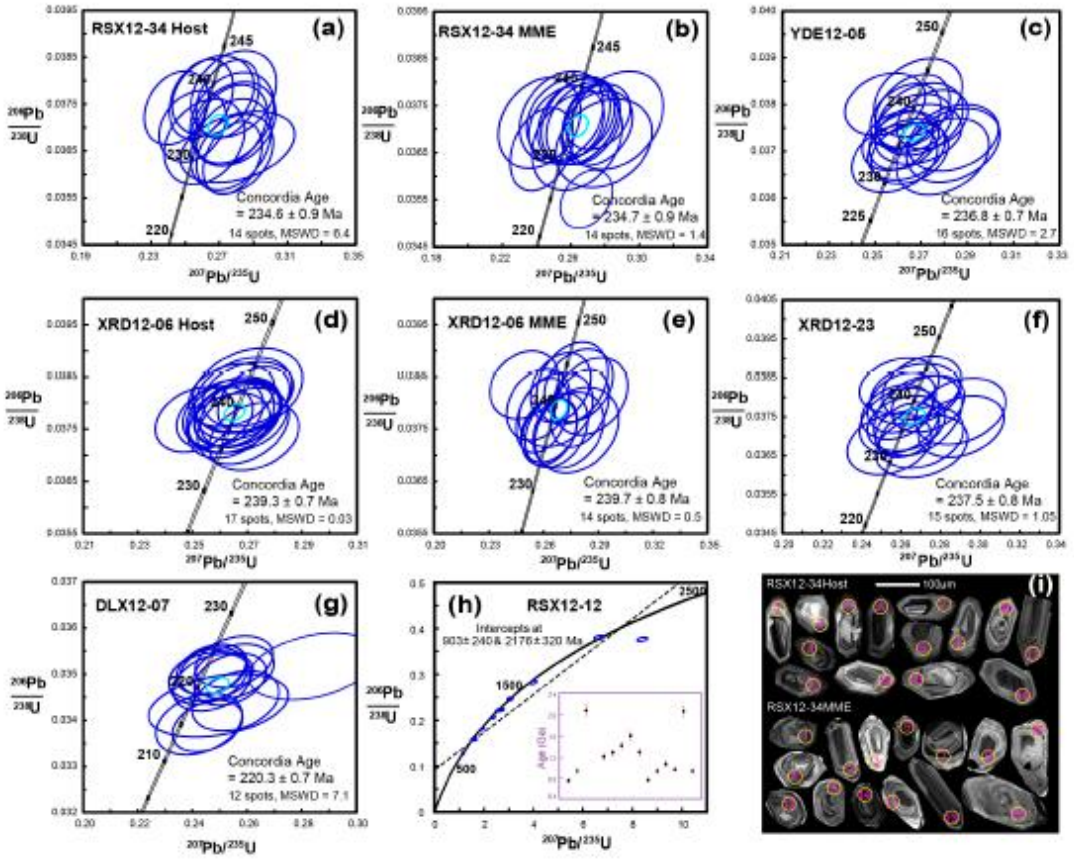

Figure 5

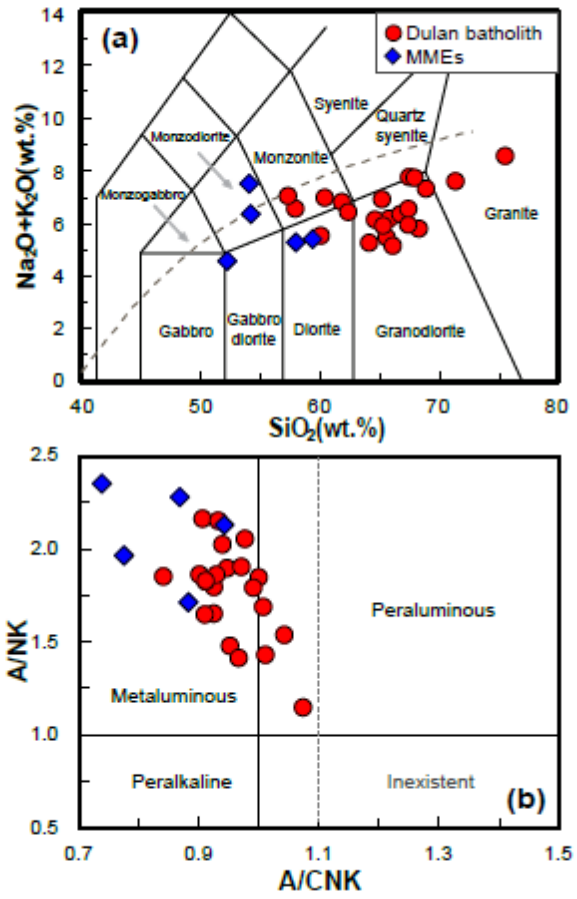

Figure 6

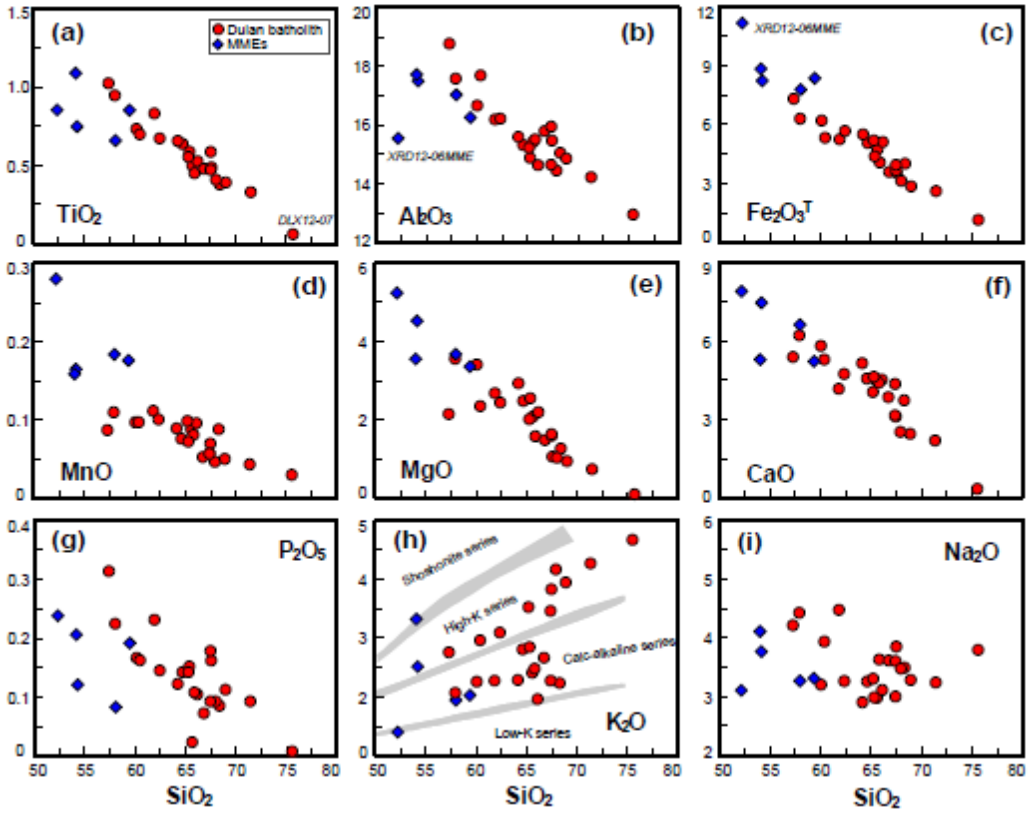

Figure 7

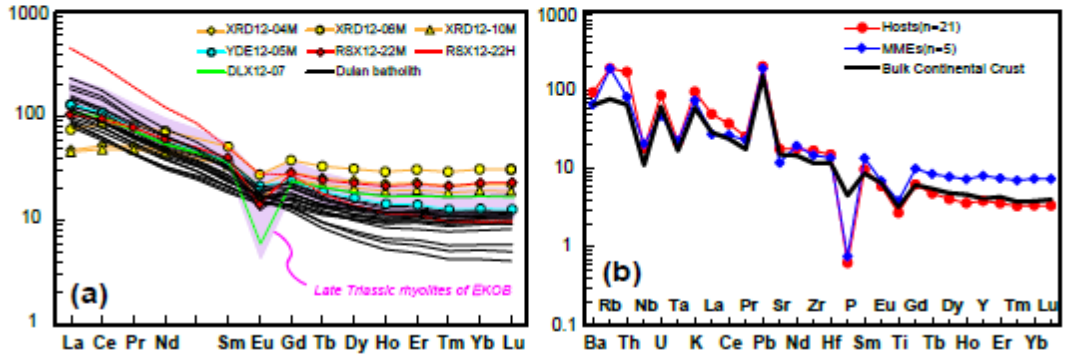

Figure 8

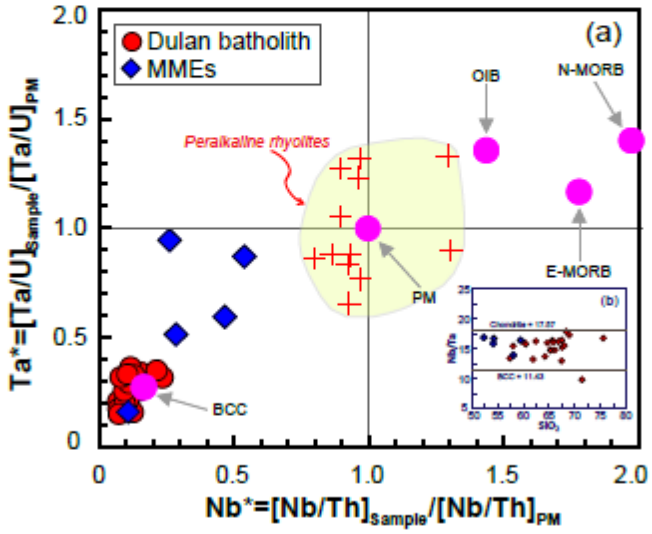

Figure 9

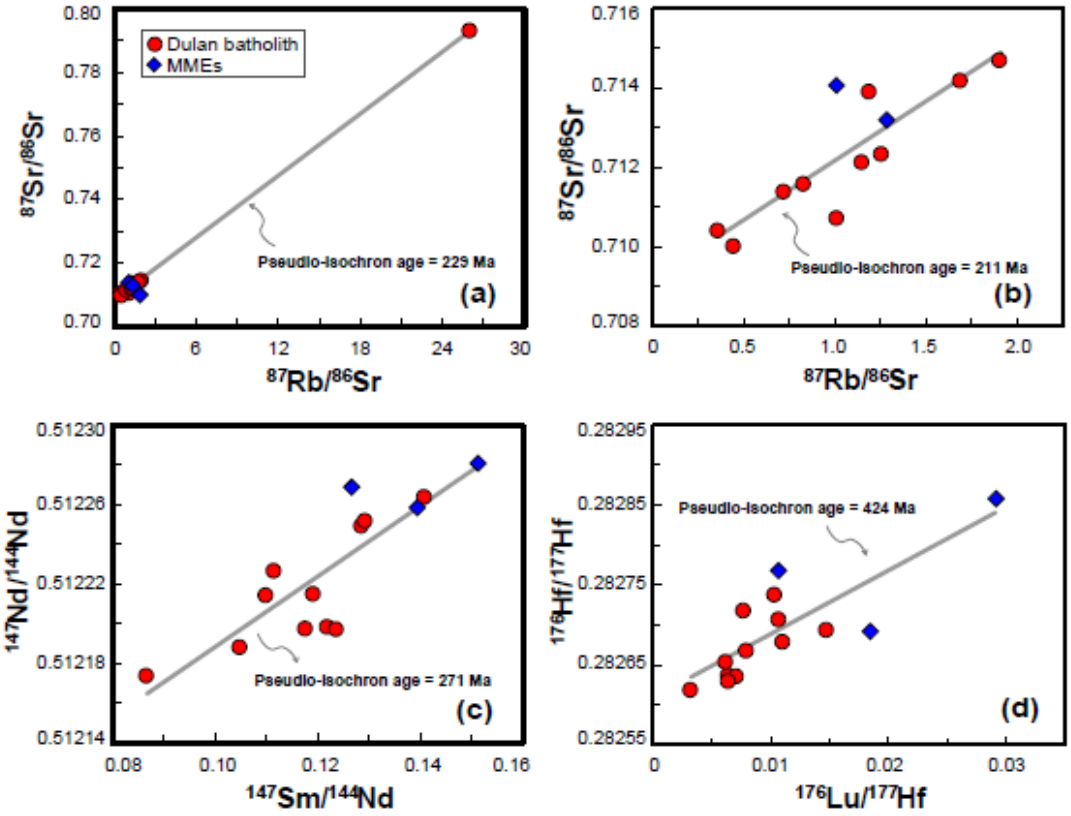

Figure 10

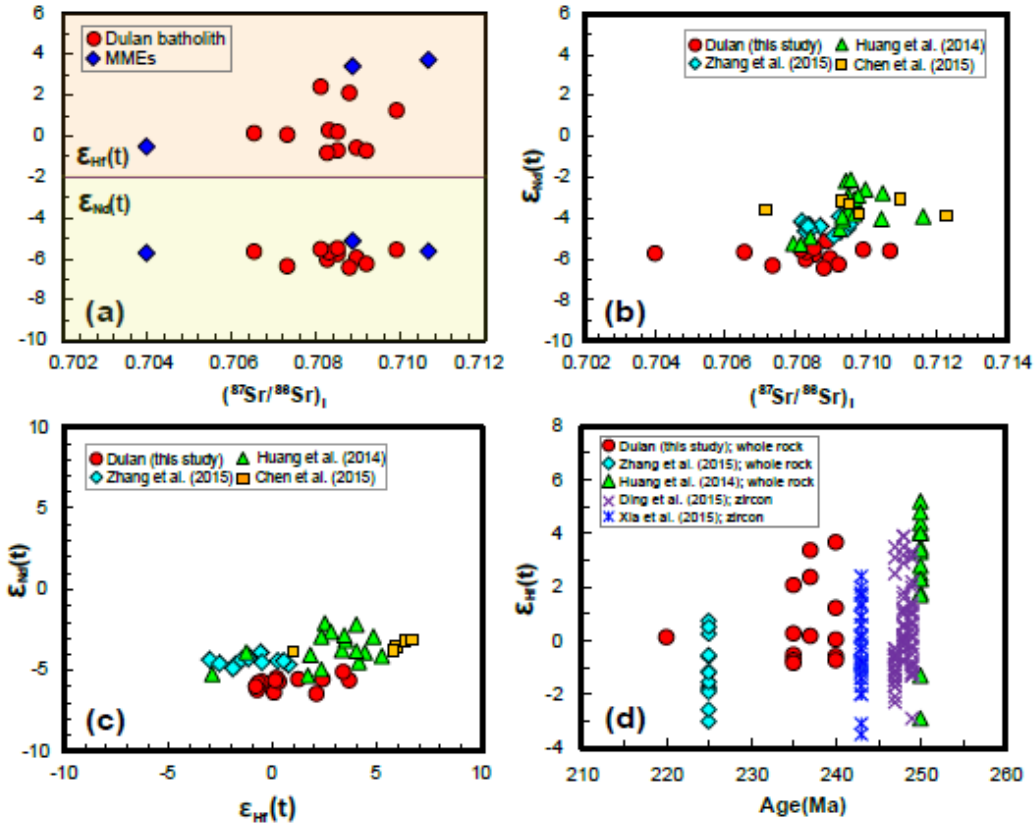

Figure 11

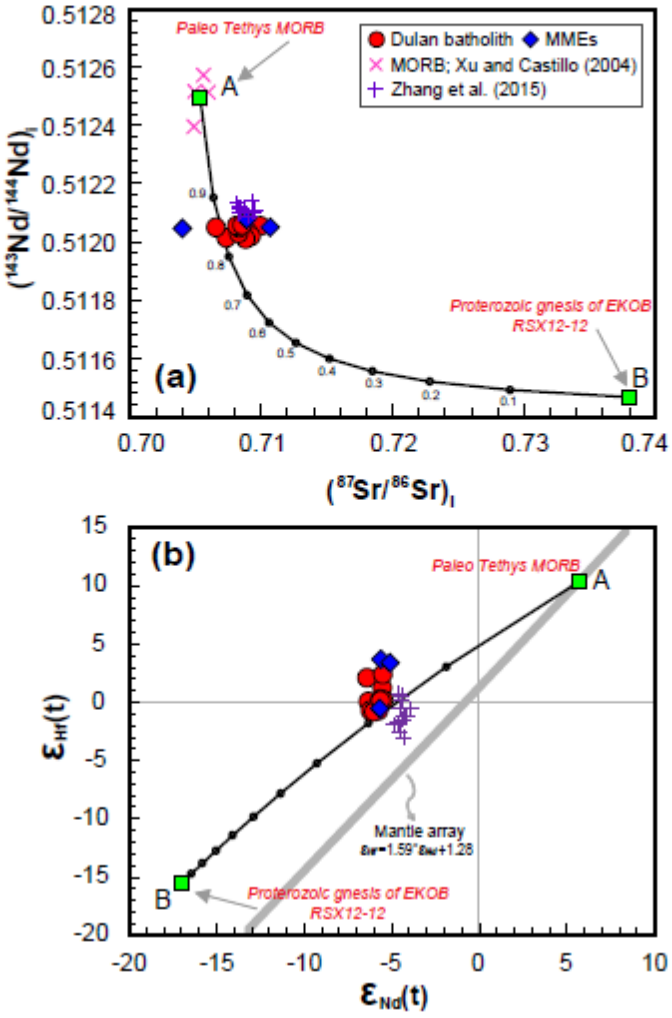

Figure 12

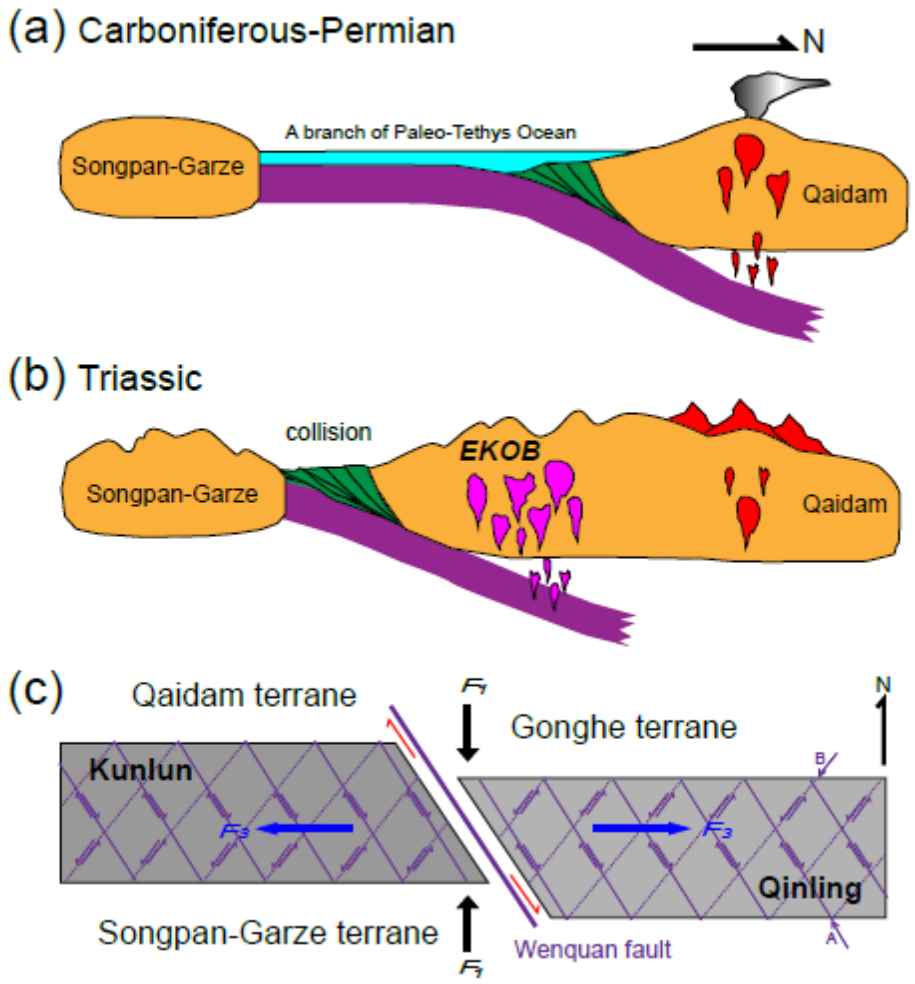

Figure 13